QUARTERLY JOURNAL OF THE ROYAL METEOROLOGICAL SOCIETY
Q. J. R. Meteorol. Soc. **135**: 1999–2011 (2009)
Published online 5 October 2009 in Wiley InterScience
(www.interscience.wiley.com) DOI: 10.1002/qj.488

Multi-event analysis of the westerly Greenland tip jet based upon 45 winters in ERA-40

Kjetil Våge,[a,b]* Thomas Spengler,[b] Huw C. Davies[b] and Robert S. Pickart[a]
[a] *Woods Hole Oceanographic Institution, Massachusetts, USA*
[b] *Institute for Atmospheric and Climate Science, ETH Zurich, Switzerland*

ABSTRACT: The westerly Greenland tip jet is an intense, narrow and intermittent wind phenomenon located southeast of Cape Farewell that occurs frequently during the winter season. Using the ERA-40 reanalysis dataset, a catalogue of 586 objectively detected westerly tip jet events is compiled for the winters 1957-2002, and an analysis is undertaken of the character of the jet and its accompanying atmospheric features. It is shown that the tip jet frequency exhibits a significant positive correlation with both the NAO index and the latitude of the Icelandic Low. The peak wind speed and accompanying heat fluxes of the jet have values up to 30 m s^{-1} and 600 W m^{-2}, respectively, and are sustained for less than one day. The air parcels constituting the tip jet are shown, based upon a trajectory model and the ERA-40 dataset, to have a continental origin, and to exhibit a characteristic deflection and acceleration around southern Greenland. The events are almost invariably accompanied both by a notable coherence of the lower-level tip jet with an overlying upper-level jet stream, and by a surface cyclone located to the lee of Greenland. It is also shown that the cyclone originates upstream of and is advected to the lee of Greenland, and thereby it both precedes in time and contributes dynamically to the formation of the tip jet. On this basis, it is suggested that the tip jet arises from the interplay of the synoptic-scale flow evolution and the perturbing effects of Greenland's topography upon the flow. Copyright © 2009 Royal Meteorological Society

KEY WORDS cyclone; jet stream; Irminger Sea; Greenland; tip jet

Received 22 January 2009; Revised 3 July 2009; Accepted 6 July 2009

1. Introduction

Greenland exerts a significant impact on the atmospheric circulation of the Northern Hemisphere. Among other things, it is known to cause a southward shift of the North Atlantic storm track (Petersen *et al.*, 2004). Both the orography and sharp low-level temperature gradients arising from the warm interior ocean adjacent to the cold water and ice on the east Greenland shelf partially account for the presence of the Icelandic Low (Tsukernik *et al.*, 2007). On shorter time-scales, numerical simulations have shown that the high topography of Greenland affects synoptic storm systems in its vicinity (e.g. Kristjánsson and McInnes, 1999; Petersen *et al.*, 2003).

The region near Cape Farewell (the southern tip of Greenland) is the windiest area of the World Ocean (Sampe and Xie, 2007). This is to a large extent due to a variety of intense, small-scale wind phenomena that arise from the impact of the Greenland topography on low pressure systems that pass nearby. (Such orographically induced winds are not unique to Greenland, e.g. Schwerdtfeger 1975; Parish, 1982; McCauley and Sturman, 1999; Seefeldt and Cassano, 2008). Near Greenland these phenomena predominantly occur in winter. Most notable are westerly (forward) and easterly (reverse) tip jets and barrier winds. Tip jets are narrow, intermittent wind patterns near the southern tip of Greenland, while barrier winds are a geostrophic response to stable air being forced towards the high eastern coast of Greenland (Moore, 2003; Moore and Renfrew, 2005; Petersen *et al.*, 2009). The focus of this study is on the westerly tip jet (Figure 1), hereafter referred to simply as a 'tip jet'.

Tip jets often develop when a low pressure system moves into the region east of southern Greenland (Moore, 2003; Pickart *et al.*, 2003a). Two mechanisms generating the tip jet have been proposed: The first involves orographic descent. Doyle and Shapiro (1999) argued that the tip jets are governed by conservation of the Bernoulli function when air parcels descend sharply down the lee slope of Greenland. (The Bernoulli function is the sum of enthalpy, kinetic energy, and potential energy per unit mass; Schär, 1993). The second mechanism, also noted by Doyle and Shapiro (1999) and later expanded upon by Moore and Renfrew (2005), involves blocking due to the high topography of Greenland. The dynamical parameter space governing the occurrence of blocking in the case when stratified flow encounters a topographic barrier has been investigated both in the absence (Smith, 1989; Ólafsson and Bougeault, 1996) and presence (Pierrehumbert and Wyman, 1985; Petersen *et al.*, 2003) of rotation (Doyle and Shapiro, 1999, provide a theoretical overview). Moore and Renfrew (2005) found that acceleration through deflection of surface winds around the

*Correspondence to: Kjetil Våge, MS#21, Woods Hole Oceanographic Institution, Woods Hole, MA 02543, USA. E-mail: kjetil@whoi.edu

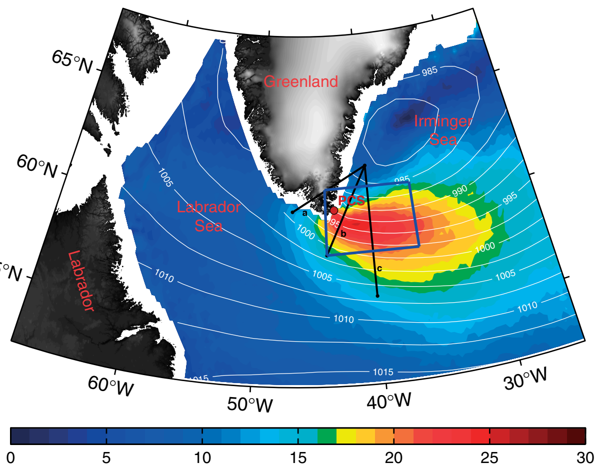

Figure 1. Mean tip jet QuikSCAT winds (colour, m s^{-1}) and ERA-40 sea level pressure (contours, hPa) over the period 1999–2002. See text for explanation of rectangle and lines. The red dot marks the location of the Prins Christian Sund (PCS) meteorological station near Cape Farewell. The Labrador Sea to the southwest and the Irminger Sea to the southeast of Greenland are regions of dense water formation.

southern tip of Greenland during periods of blocking was a consistent feature of tip jets in their climatological study of high wind speed events in the vicinity of Greenland.

The small meridional scale of the tip jet results in a region of localized high cyclonic wind-stress curl east of Cape Farewell (Pickart *et al.*, 2003a). Using an idealized ocean model, Spall and Pickart (2003) showed that this patch of enhanced wind-stress curl is sufficient to drive the recirculation gyre observed in the Irminger Sea east of Greenland (Lavender *et al.*, 2000). The cyclonic wind-stress curl leads to upwelling and isopycnal doming in the water column below, which, together with the large heat fluxes caused by the strong winds, are conducive for driving deep oceanic convection in winter (Pickart *et al.*, 2003a; Våge *et al.*, 2008). It has been hypothesized that the southwestern Irminger Sea, within the Irminger Gyre and under the direct influence of the tip jet, may be another region where the densest type of subpolar mode water, Labrador Sea Water (LSW), is formed during sufficiently severe winters (Pickart *et al.*, 2003b). (LSW was previously thought to originate solely from the Labrador Sea.) The strong tip jet winds also present a significant marine hazard (e.g. Moore, 2003).

In this work we use an objective and sensitive method to explore the ERA-40 meteorological reanalysis product for the signatures of tip jets. The goal is to form a comprehensive and consistent climatology of such events, which is then used to investigate the evolution of the tip jet and to gain further dynamical insight regarding its mechanism of generation. The main advantages of using a meteorological reanalysis for climatological studies are the long time periods covered and the availability of all relevant meteorological fields on a three-dimensional grid, while the main disadvantage is a relatively coarse horizontal and vertical resolution. The advent of satellite scatterometers (in particular the QuikSCAT satellite in 1999), which measure the surface wind field over the ocean at high resolution, provides an opportunity to check the consistency of the lower-resolution reanalysis surface winds in the vicinity of Cape Farewell.

The paper is outlined as follows. The ERA-40 reanalysis product and the tip jet detection routine are described in section 2. A comparison with the QuikSCAT satellite scatterometer winds follows in section 3. In section 4 the relationship between tip jet frequency and large-scale North Atlantic atmospheric patterns are examined. Composite averages provide a robust description of the evolution of the tip jet and are described in section 5. A Lagrangian trajectory analysis, presented in section 6, complements the description of the tip jet by identifying the paths and origin of the air parcels contained within the jet. The atmospheric conditions during tip jet events are investigated in section 7. In section 8 we discuss the dependency of the tip jet on the low-level flow interaction with the topography of Greenland as well as on the large-scale atmospheric conditions.

2. Data and methods

2.1. ERA-40 reanalysis product

The European Centre for Medium-Range Weather Forecasts (ECMWF) 45-year reanalysis product (ERA-40; Uppala *et al.*, 2005) covering the period 1957 to 2002 was analyzed in this study. The horizontal and temporal resolutions at the surface and at 23 pressure levels are 1° and 6 h, respectively. Produced with a fixed numerical weather prediction data assimilation system, ERA-40 (and other reanalysis products) provides a physically consistent interpolation of historical observational data through space and time. However, the observing system did not remain constant during this period. The growing importance of satellite instruments after 1979 had a particularly large impact on the meteorological analyses, mainly in regions where ground-based observations were sparse and in the upper troposphere and stratosphere (Bengtsson *et al.*, 2004). Thus the ERA-40 fields may not be regarded as fully consistent throughout the entire period. For our tip jet climatology this issue is not addressed, but it is less of a concern in the Northern Hemisphere. Furthermore, upper-level atmospheric data are only considered for the most recent period.

As a check on the accuracy of the ECMWF model in a subpolar region of sparse data, Renfrew *et al.* (2002) compared the surface fields from the National Centers for Environmental Prediction (NCEP; Kalnay *et al.*, 1996) and the ECMWF operational analysis with data recorded by the research vessel *Knorr* during a 1997 winter cruise in the Labrador Sea. They found that the ECMWF model fields represented the observed data reasonably well, but contained a cold bias for sea surface temperature and 2 m air temperature near the ice edge, and a tendency to overestimate the latent and sensible heat fluxes. In the present study the latter issue is circumvented to some extent by application of a bulk formula (Fairall *et al.*, 2003) to compute the heat fluxes in section 5.

Concerns regarding the ability of a global product of relatively coarse resolution like ERA-40 to accurately

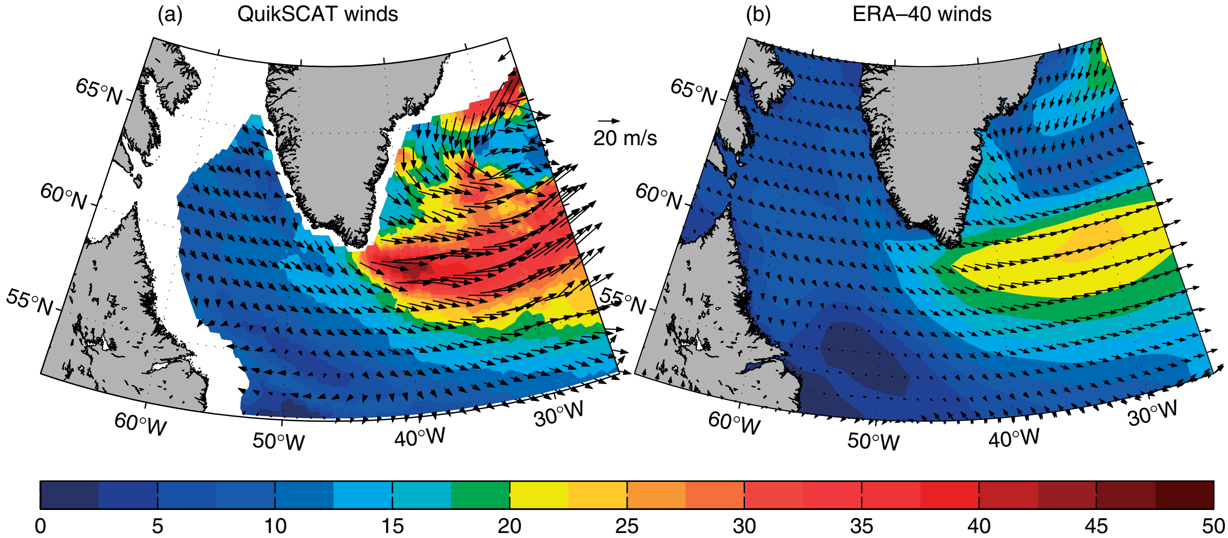

Figure 2. Surface wind field (m s^{-1}) during the 21 February 2002 tip jet event, illustrating the difference between (a) QuikSCAT and (b) ERA-40.

capture small-scale atmospheric phenomena such as the Greenland tip jet (Figure 2) have been raised previously (Moore, 2003; Pickart *et al.*, 2003a). This is examined further in section 3.

2.2. Tip jet detection

Two empirical orthogonal function (EOF) approaches have been used in previous studies to objectively detect tip jet events. Pickart *et al.* (2003a) found that tip jets were characterized by strong westerly winds, anomalously low air temperatures, and low sea level pressure. They constructed an EOF based on these three variables using nearly 30 years of meteorological data from the Prins Christian Sund weather station near Cape Farewell (labelled PCS in Figure 1) to identify the events. Våge *et al.* (2008) noted that tip jet events were relatively insensitive to the location and central pressure of their parent low pressure systems, and showed that the gradient of sea level pressure was a better metric than sea level pressure alone. Some tip jets were also observed to completely evade the meteorological station. Correspondingly, Våge *et al.* (2008) devised an EOF routine that employed time series of (i) the maximum 10 m zonal wind speed within the blue rectangle of Figure 1 recorded by the QuikSCAT satellite scatterometer (retrieved using the ‘Ku-2001’ model; Wentz *et al.*, 2001); (ii) the mean NCEP sea level pressure gradient along the lines a, b, and c in Figure 1; and (iii) the PCS air temperature. This method proved to be more sensitive to tip jet detection, and had the advantage of utilizing accurate, high-resolution satellite wind speed data covering a larger geographical area. Våge *et al.* (2008) used a threshold zonal wind speed of 25 m s^{-1} to define a robust tip jet. Manual inspection of the scatterometer winds confirmed that all of the robust tip jets that took place during the two winters that they considered were detected.

In this work we primarily use the EOF routine developed by Våge *et al.* (2008). We note that satellite scatterometers were not available prior to 1987, and that there are temporal gaps in the PCS air temperature record. Hence we use only time series extracted from ERA-40 as input for the EOF routine. ERA-40 was used alone in order to have a consistent detection algorithm covering the entire period. Furthermore it is desirable to avoid data from the location of the PCS weather station due to suspected influence of the high local topography. Instead of temperatures from the PCS location, we used a roving temperature time series. At each time step, the temperature at the location of the maximum zonal wind speed within the blue rectangle of Figure 1 was tabulated. In this way the temperature at the core of the tip jet was always considered. For completeness we also applied the same EOF method implemented by Pickart *et al.* (2003a) using the PCS data only. For the majority of cases, the two EOF routines identified the same events.

While we use the same routine as Våge *et al.* (2008), our reconstructed tip jet winds are weaker than theirs largely because of the coarser resolution of the ERA-40 winds. As such, the threshold reconstructed zonal wind speed for defining an event as robust was lowered from 25 to 18 m s^{-1}. This limit was chosen to achieve a balance between avoiding false positive identifications, and at the same time not missing robust tip jets. The threshold value was determined by carefully comparing the ERA-40 and QuikSCAT winds for the period of overlap (1999–2002). In reality there exists a continuum of tip jet magnitudes, and the label ‘robust’ is somewhat arbitrary. All tip jets discussed from this point onwards are robust according to the above definition, hence the label will be dropped.

All of the events that satisfied the criteria from either of the two EOF routines above were examined manually to ensure that each tip jet was recorded once, at its peak intensity, and to locate the centres of their parent low pressure systems. In addition to the two EOFs, a final procedure was applied to detect wind speed events

DOI: 10.1002/qj

exceeding 20 m s^{-1} with a direction deviating at most 30° from west within the blue rectangle of Figure 1. This was done to identify any events that might have been missed by the EOFs. Only a few such cases were identified. In total, 586 tip jet events were detected in the ERA-40 reanalysis for the winters (November–April) of 1957 to 2002. This is on average 13 per winter. Validation of our climatology through comparison with QuikSCAT for the period of overlap indicates that 88% of all of the tip jets that had mean QuikSCAT wind speeds within the blue rectangle in Figure 1 exceeding 25 m s^{-1} were detected in ERA-40 without reporting false positives. The tip jets found only in the QuikSCAT dataset were in general weaker and/or of shorter duration than the tip jets identified in ERA-40.

3. ERA-40 versus QuikSCAT winds

3.1. Winter conditions

To examine the correspondence between ERA-40 and QuikSCAT winds, the mean 10 m wind speed within the blue rectangle of Figure 1 was determined for every realization of each dataset during the winters of overlap (1999–2002). The ERA-40 time series was then temporally interpolated onto the same twice-daily time base as the QuikSCAT data (Figure 3(a)). The correlation between the wind speeds from the two products in this region is 0.89. All correlations reported are significant at the 99% confidence level. (Confidence intervals were determined using a bootstrap algorithm, a procedure that involves random sampling with replacement from the dataset and does not require any assumptions about the underlying probability distribution.) The linear least-squares best fit resulted in the following relation between the two wind speed products:

$$|\mathbf{v}|_{\text{QuikSCAT}} = 1.4|\mathbf{v}|_{\text{ERA-40}} - 0.9. \quad (1)$$

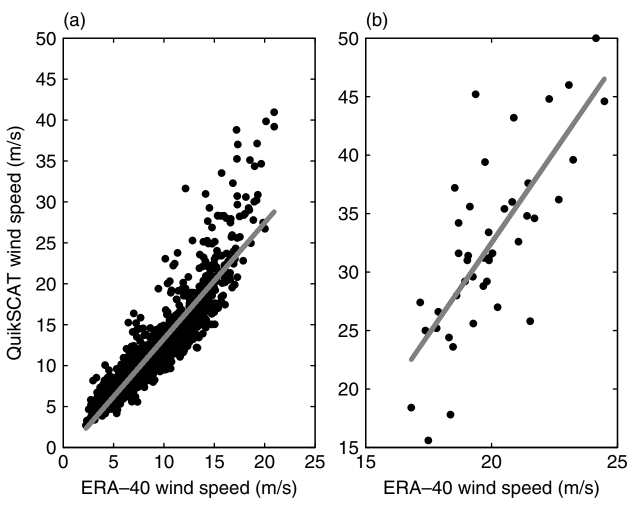

Figure 3. Relationships between (a) mean ERA-40 and QuikSCAT 10 m wind speeds (m s^{-1}) within the blue rectangle of Figure 1 twice daily during all of the winters of overlap and (b) maximum ERA-40 and QuikSCAT 10 m wind speeds found within the same box during tip jet events (43 events in total).

In the region near Cape Farewell, the ERA-40 and QuikSCAT winds are generally well correlated, but the good correlation tends to break down for the highest wind speeds. In particular, all of the QuikSCAT wind speeds exceeding 30 m s^{-1} were associated with small-scale wind events: westerly and easterly tip jets and barrier winds. As mentioned in the introduction, these wind phenomena result from the impact of the high topography of Greenland on a nearby low pressure system, and it is clear that they are not as well represented in the lower-resolution ERA-40 fields. However, Moore *et al.* (2008) found that, relative to a meteorological buoy in the Irminger Sea, QuikSCAT showed evidence of a high wind speed bias. Renfrew *et al.* (2009) reached a similar conclusion using aircraft-based observations east of southern Greenland. This bias may be a contributing factor to the reduced correlation at extreme wind speeds, though the underestimation of high winds in ERA-40 due to low resolution and orographic effects is likely the dominant reason.

3.2. Tip jet conditions

Considering only the wind speeds during tip jet events, the correlation between ERA-40 and QuikSCAT maximum wind speeds dropped to 0.75 (Figure 3(b)), and the least-squares relation changed to

$$|\mathbf{v}|_{\text{QuikSCAT}} = 3.1|\mathbf{v}|_{\text{ERA-40}} - 30. \quad (2)$$

We chose to consider the maximum wind speed instead of the mean because the scale of the tip jet is much smaller than the rectangle. (When considering the mean wind speed during tip jet events, the correlation was 0.78.) We will also use Equation (2) to estimate the 'true' wind speed at the core of the composite average tip jet in section 5.

It is clear that ERA-40 significantly underestimates the wind speeds during tip jet events relative to the scatterometer. Using the global ECMWF forecast model, Jung and Rhines (2007) found that increasing the model resolution beyond that of ERA-40 continuously improved the representation of the tip jet as judged by high-resolution scatterometer studies of the tip jet (Moore and Renfrew, 2005). In particular, both the heat flux and surface wind-stress curl were increased. In any case, the significant positive correlation between ERA-40 and QuikSCAT winds during tip jet events indicates that our tip jet climatology effectively captures the most intense tip jet events.

4. Tip jets and the NAO

The North Atlantic Oscillation (NAO) is the dominant pattern of climate variability in the North Atlantic (Hurrell, 1995). Winters that are characterized by a positive NAO index are associated with stronger westerly winds, enhanced air–sea buoyancy fluxes, and are often linked with deep convection in the subpolar North Atlantic

DOI: 10.1002/qj

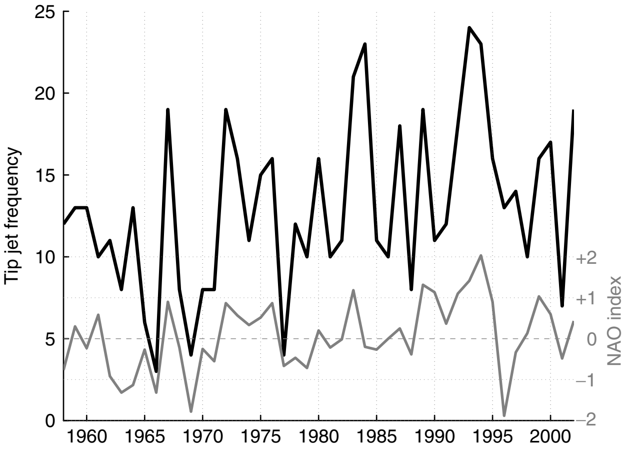

Figure 4. Time series of winter tip jet frequency (black) and NAO index (grey).

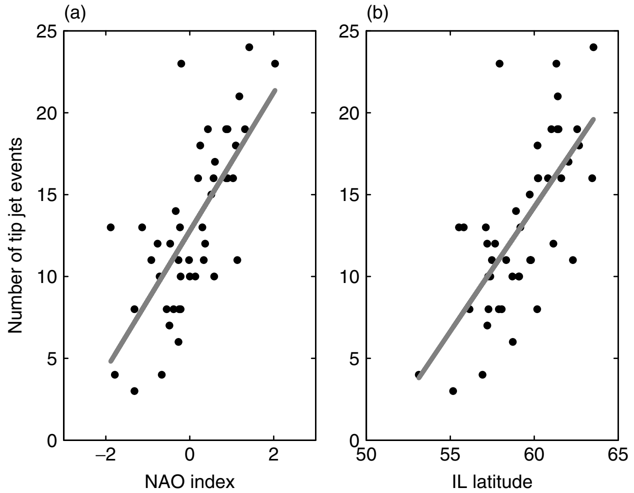

Figure 5. Relationships between winter tip jet frequency and (a) the NAO index and (b) the latitude of the Icelandic Low.

Ocean (Dickson *et al.*, 1996; Våge *et al.*, 2009). Pickart *et al.* (2003a) also found that a greater number of tip jet events took place during high NAO index winters. Figure 4 shows the time series of winter (Nov–Apr) tip jet frequency over the 45-year period of ERA-40. Significant interannual variability is evident; some winters have as few as 3–5 tip jets, while others have as many as 20–25. On average, there are 13 tip jet events per winter, with a standard deviation of 5. Figure 4 also illustrates the temporal relation between tip jet frequency and the monthly NAO index of Hurrell (1995) averaged over the winter months (Nov–Apr). Using the tip jet climatology of Pickart *et al.* (2003a) and the atmospheric NAO pattern decomposed into indices of Icelandic Low (IL) and Azores High (AH) centres of actions (COA; Hameed *et al.*, 1995), Bakalian *et al.* (2007) found that the number of tip jet events per winter was more sensitive to the latitude of the IL than to the NAO index.

Using the present climatology, with the monthly NAO index of Hurrell (1995) and the COA indices of Hameed *et al.* (1995) averaged over the winter months (Nov-Apr), we find similar correlations. This is true despite the under-represented tip jet frequency in Pickart *et al.* (2003a)'s climatology (Våge *et al.*, 2008). In particular, we find correlations of 0.71 and 0.69 between the number of tip jet events per winter and the NAO index and latitude of the IL, respectively. This suggests that the NAO state and the meridional location of the IL are of comparable importance for the frequency of tip jet events (Figure 5). As the location of the IL may influence the value of the station-based NAO index, these variables are not expected to be completely independent. Indeed, a correlation of 0.86 was found between the NAO index and the latitude of the IL. Using the wintertime NAO index (Hurrell, 1995) based upon the months December to March, the correlation decreased to 0.64. (A similarly low correlation of 0.65 was obtained when averaging the monthly NAO index over the same months.) This shows that the shoulder months, November and April, which are important from an oceanic convection perspective, also contribute a sizeable number of tip jet events (16% and 8%, respectively).

5. Tip jet composites

Composite averages of all 586 tip jets from the ERA-40 dataset during the 24 h period surrounding an event portray the tip jet as an intense, short-lived phenomenon (Figure 6). Peak wind speeds approaching 20 m s^{-1} were sustained for less than a day (Figure 6(a)). Pickart *et al.* (2003a) found that tip jets at the PCS meteorological station on average lasted approximately 3 days. The discrepancy between these estimates of tip jet duration is mainly due to our focus on peak tip jet wind speeds, while they also considered the shoulders of the tip jet events. Using Equation (2), the 'true' wind speed at the core of the composite average tip jet was estimated to exceed 30 m s^{-1}. The region of low sea level pressure localized northeast of Cape Farewell was at its deepest and most compact at the peak of the tip jets (Figure 6(b)), and at a lag of +12 h had moved in the downstream direction towards Iceland. This is reflected in the gradient of sea level pressure. The strong pressure gradient extending eastward from Cape Farewell, which in agreement with Våge *et al.* (2008) was found to be a feature common to every tip jet event, was most intense at the peak of the composite event compared to lags ± 12 h. This is consistent with the composite velocities (Figure 7(a)). In agreement with previous studies (e.g. Pickart *et al.*, 2003a), every tip jet event was associated with a parent low pressure system (marked with an L in Figure 6(b)). Although most of the parent cyclones were located close to the east coast of Greenland, there was a significant scatter in their positions, but never to the extent that the strong pressure gradients east of Cape Farewell were compromised.

Turbulent heat fluxes were computed using a bulk formula (COARE 3.0; Fairall *et al.*, 2003) with the inputs of wind speed, humidity, air temperature and sea surface

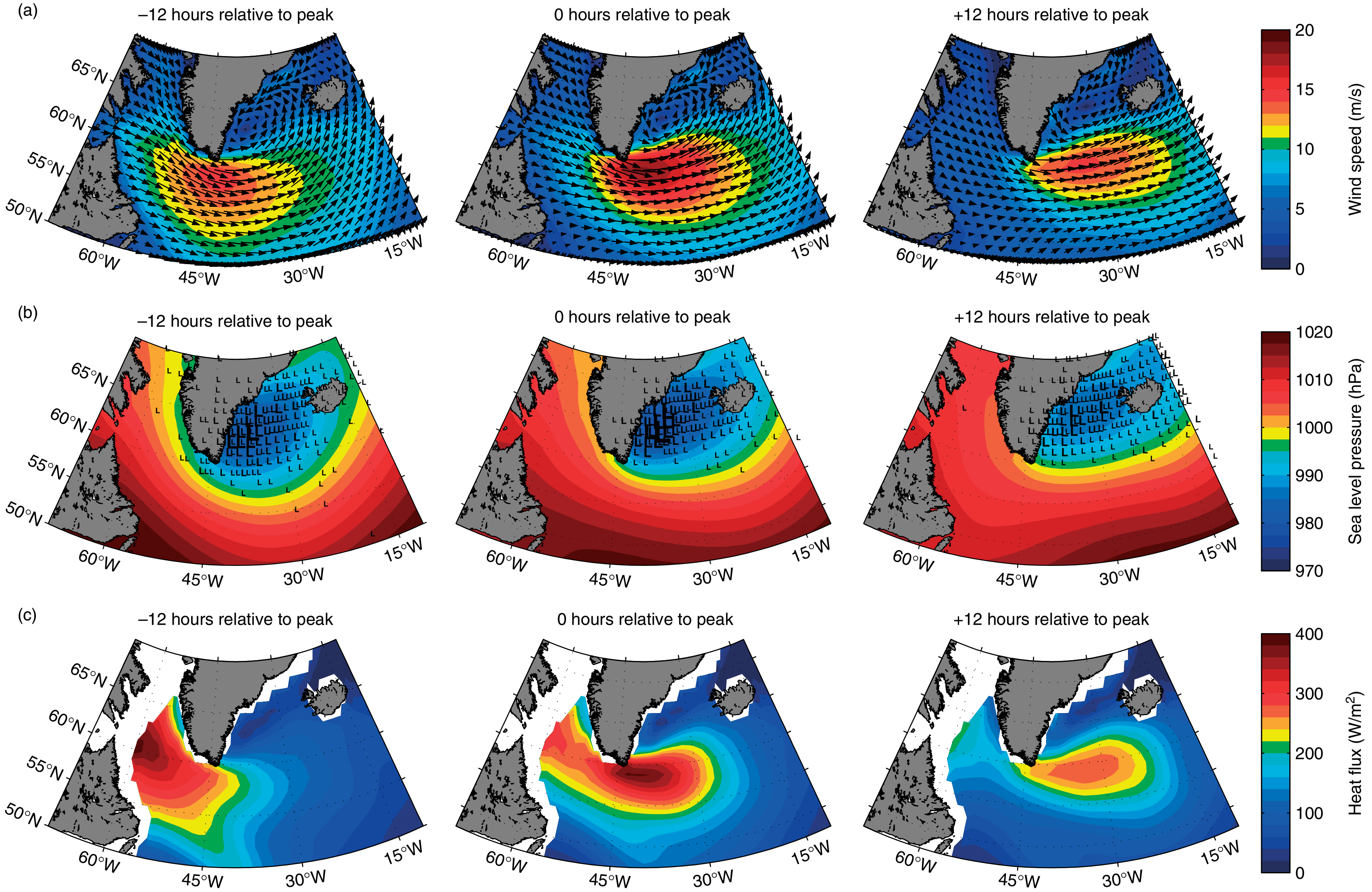

Figure 6. Composite averages of (a) wind speed (m s^{-1}), (b) sea level pressure (hPa), and (c) turbulent heat fluxes (W m^{-2}) illustrating the temporal evolution of the Greenland tip jet. The title of each panel refers to the time lag relative to the peak of the composite tip jet. The Ls in (b) indicate the locations of the centres of the parent cyclones, and the sizes of the Ls are proportional to the number of cyclones they represent.

temperature, and were on average more than three times greater during tip jet events than background levels (Figure 6(c)). Replacing the ERA-40 wind speed with our estimate of the true wind speed in the bulk formula raised the heat fluxes in the centre of the composite tip jet from 400 W m^{-2} to almost 600 W m^{-2}. Even though the QuikSCAT-based true wind speed estimate may have a positive bias (Moore *et al.*, 2008; Renfrew *et al.*, 2009), the magnitude of the heat flux at the core of the tip jet is still likely to be underestimated. Tip jets are associated with a drop in air temperature (Pickart *et al.*, 2003a), and it will be shown in section 6 that cold, low-humidity air of continental origin tends to comprise the tip jets. Neither of these features are well captured by the ERA-40 dataset, and both would tend to further increase the tip jet heat fluxes. This suspected heat flux underestimate is also consistent with the case-studies of Jung and Rhines (2007).

As seen in Figure 6(c), large heat fluxes are also present over the Labrador Sea 12 h prior to the peak of the tip jet events. These are most likely associated with cold air outbreaks, during which low pressure systems following the North Atlantic storm track draw cold and dry continental air from Labrador over the relatively warm ocean, thereby enhancing the air–sea heat fluxes (e.g. Pickart *et al.*, 2008). The analysis of Våge *et al.* (2009) shows that the very same storms that cause cold air outbreaks in the Labrador Sea tend to trigger tip jet events a few hours later as they progress northeastward along the storm track. Both of these locations of high heat fluxes, the western Labrador Sea and the southwestern Irminger Sea, are regions where deep convection is known to take place during severe winters. For the evolution of the oceanic mixed layer in the Irminger Sea, the integrated effect of many tip jets during the course of a winter is of great importance (Våge *et al.*, 2008).

6. Air parcel trajectories

To better understand the potential impact of tip jets on oceanic convection, it is necessary to know the origin of the air that they transport. Cold and dry continental air will extract more heat from the ocean than relatively warm and moist maritime air. The upstream path of air parcels comprising the tip jets might also provide evidence supporting one of the proposed mechanisms of formation; i.e. either the orographic descent hypothesis of Doyle and Shapiro (1999) or the acceleration through deflection hypothesis advocated by Moore and Renfrew (2005).

A three-dimensional Lagrangian trajectory model (Wernli and Davies, 1997) was applied to compute 2-day backwards air parcel trajectories terminating above the southwestern Irminger Sea (900 to 950 hPa) using ERA-40 winds as input. Only trajectories from the core of each tip jet were included, selected objectively by requiring the wind speed to exceed 20 m s^{-1} and the direction to deviate no more than 30° from west at the point of termination. Given the evolving observing system (Bengtsson *et al.*, 2004) and computation constraints, only the most recent winters (1994 to 2002) were considered for this analysis, resulting in nearly 3000 trajectories from 101 tip jet events (Figure 7).

The trajectories so computed clearly illustrate the continental origin of the air parcels constituting the tip jet. This has important implications for the air–sea heat exchange in the Irminger Sea, as the air originating from northern Canada in winter is usually very cold and dry. Before reaching the Irminger Sea, the air must cross the Labrador Sea, whose western margin and northern end are covered with ice in winter. Hence modification by air–sea interaction in the Labrador Sea is somewhat reduced, and, as shown in section 5, tip jets are very effective at extracting heat from the southwestern part of the Irminger Sea. A marked difference in origin of the air comprising the westerly and easterly tip jets is likely a major reason why the latter is not believed to cause deep oceanic convection in the southeastern Labrador Sea (Sproson *et al.*, 2008).

Figure 7 also demonstrates that most of the trajectories curve around Greenland, suggesting that acceleration by deflection is a key mechanism of tip jet generation (e.g. Moore and Renfrew, 2005). In order to shed more light on this, the pressure change and velocity along each trajectory were computed and interpolated onto a 0.5° × 0.5° grid using a Laplacian-spline interpolator. The resulting along-trajectory pressure change (Figure 8(a), colour) indicates that some sinking takes place over southern Greenland, which would support the orographic descent under Bernoulli conservation hypothesis of Doyle and Shapiro (1999). However, this involves only a small number of trajectories; less than 18% of the trajectories experienced a temporal pressure change greater than 25 hPa h^{-1} (Figure 8, contours). The vast majority of the trajectories pass to the south of Cape Farewell, and the acceleration associated with deflection around Greenland is evident (Figure 8(b), colour).

The mean Froude number estimated west of Greenland during tip jet events is much less than 1. (The Froude number is computed as $Fr = U/NH$, where U is wind speed, N is buoyancy frequency (a measure of static stability), and H is the obstacle height. U and N were computed from the ERA-40 climatology upstream and below the height of the obstacle, which was taken to be 2500 m.) This indicates that stratification dominates the inertia of the air parcels, and hence the air is more likely to flow around than over Greenland (Skeie *et al.*, 2006). This corroborates the evidence from the trajectory model.

7. Flow features accompanying the tip jet

To improve our understanding of the processes leading to the formation of tip jets, we examine the major atmospheric flow features that accompany these events and how they relate to the results from the air parcel trajectory model. In particular we focus on the low-level cyclones and the tropopause-level jet stream.

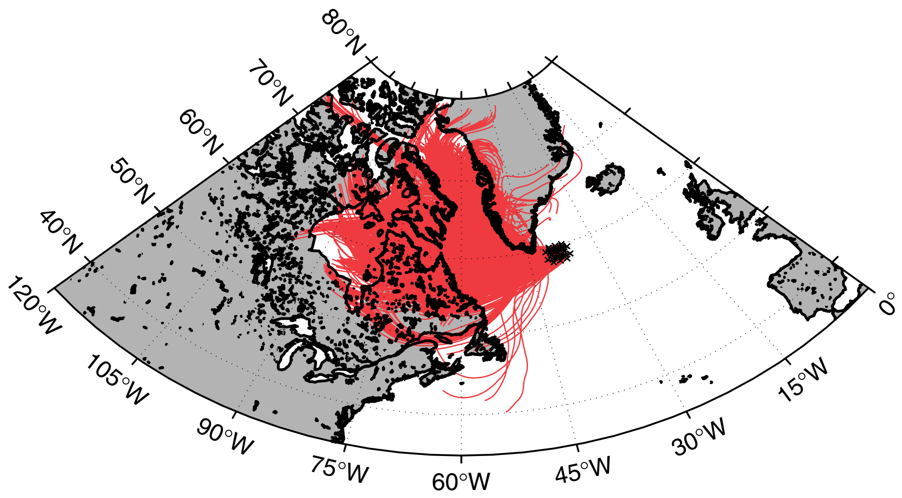

Figure 7. Backward 2-day trajectories of air parcels within tip jets (see text for selection parameters). Note the continental origin of the air composing the tip jet and how the trajectories curve around southern Greenland.

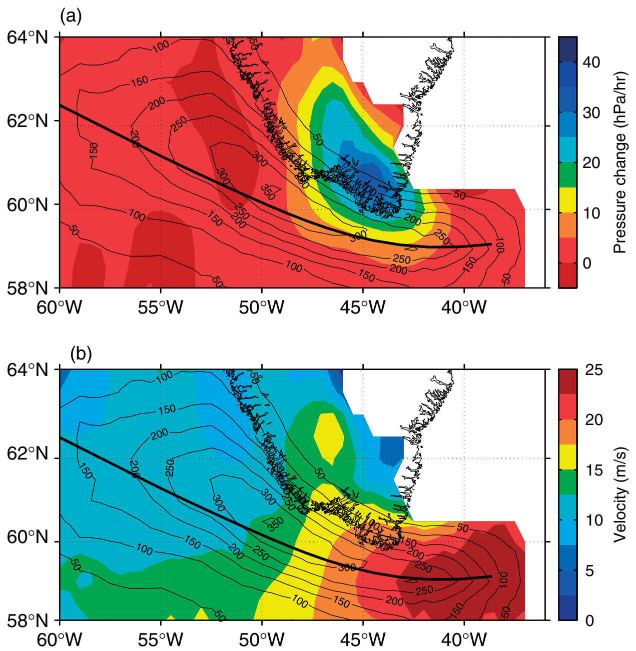

Figure 8. (a) Pressure change (hPa h^{-1}) and (b) velocity (m s^{-1}) computed along the trajectories from Figure 7. The contours denote the number of realizations, and the black line marks the mean tip jet trajectory.

7.1. Low-level cyclone

It was noted earlier that the synoptic-scale flow incident upon Greenland can generate numerous small-scale weather phenomena (Renfrew *et al.*, 2008, provides an overview). Here we examine the occurrence and nature of the low-level cyclonic systems that appear to be ubiquitous accompanying features of tip jets. The aim is to shed light upon the relationship between the cyclone and the tip jet. To this end we use a database (Wernli and Schwierz, 2006) that identifies the storm tracks and cyclone field (defined as the area within the outermost closed 2 hPa pressure contour of a low pressure system) based upon the ERA-40 reanalysis sea level pressure data. To select the cyclones that were associated with tip jet events from the database, we matched their spatio-temporal locations with the manually determined positions of the tip jets' parent low pressure systems. A success rate of 98% testifies to the robustness of the database.

Consider in turn the storm track and the along-track pressure change and speed of translation of the subset of ERA-40 cyclones that were associated with tip jet events. For the tracks (Figure 9) it is evident that most of the cyclones linked to the occurrence of tip jets followed a well-defined path from the eastern seaboard of North America into the Irminger Sea. A similar picture emerged from the manually tracked parent low pressure systems for the two individual winters of 2002–2003 and 2003–2004 analyzed by Våge *et al.* (2008), and is also consistent with the results of Hoskins and Hodges (2002).

The pre-existence of the cyclonic systems prior to their arrival over the Irminger Sea has important ramifications. It demonstrates that the cyclogenesis that spawns these systems tends to occur upstream of Greenland rather than being an example of *in situ* lee cyclogenesis off southern Greenland (e.g. Jung and Rhines, 2007; Kristjánsson and Thorsteinsson, 2009; McInnes *et al.*, 2009). Consequently it suggests that orography alone does not produce the conditions necessary for tip jet formation, and that the upstream synoptic-scale flow evolution plays an important role as well.

To examine these issues further, consider the pressure change and translation speed of these systems (Figure 10) computed along each cyclone's track in the same manner as the along-trajectory evolution in section 6. These patterns show that the mean behaviour of the cyclones was to deepen while rapidly approaching Greenland from the southwest, and thereafter decelerate and start to fill as they traverse the Irminger Sea and migrate toward Iceland. The large translation speeds northwest of Iceland in Figure 10(b) reflects a tendency of a substantial subset of cyclones to rapidly transit through the Denmark Strait separating Greenland and Iceland. These features both indicate that the storms were spawned upstream and

DOI: 10.1002/qj

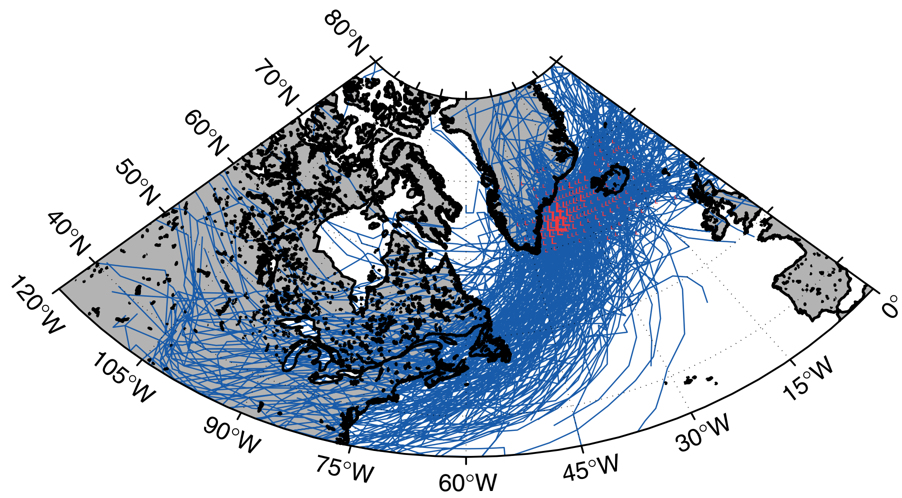

Figure 9. Tracks of tip jet-generating cyclones for the duration of their existence. The Ls mark the locations of the centres of the parent cyclones at the peak of each event, with the size proportional to the number of cyclones represented.

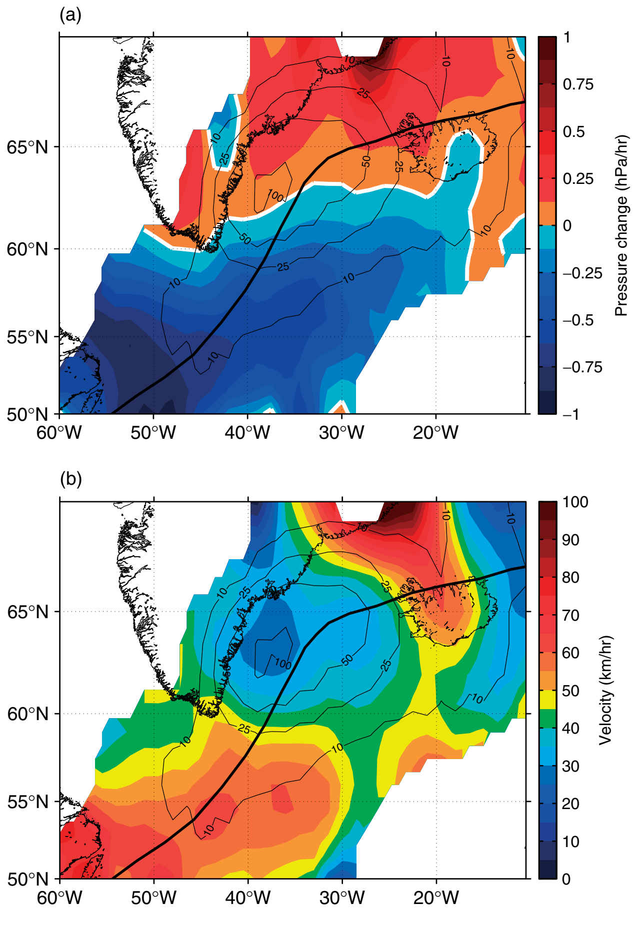

Figure 10. (a) Pressure change (hPa h^{-1}) and (b) translation speed (km h^{-1}) computed along the storm tracks from Figure 9. The contours indicate the number of realizations, the black line denotes the mean path of the cyclones, and the white line in (a) is the zero contour.

de-emphasize the role of lee-cyclogenesis, either acting in isolation or in tandem with the synoptic development, on the subset of low pressure systems associated with tip jet events. Also, the decrease in translation speed of the systems between Greenland and Iceland (Figure 10(b) and Hoskins and Hodges, 2002) is consistent with this, suggesting that many of the cyclones are 'captured' in the lee of Greenland (Jung and Rhines, 2007) and that their slow translation may be a contributing factor to the formation of the semi-permanent Icelandic Low.

7.2. Vertical structure of the tip jet and relationship to the jet stream

Further consideration of the ambient synoptic-scale flow is prompted by the finding that its evolution plays a significant role in the development of the tip jet. A key component of that ambient flow is the tropopause-level jet stream, and to depict its character Figure 11 shows the composite average wind speed for the recent subset (1994–2002) of tip jet events. In these depictions the tip jet itself is evident as the laterally confined, low-level band of strong wind speed south and east of Cape Farewell, and is associated with comparatively small case-to-case variability. The jet stream corresponds to the broader and more elongated band of strong winds at upper levels located slightly more towards the Equator. A similar structure to this composite was observed for a single tip jet event during a November 2003 aircraft flight equipped with dropsondes and an airborne Doppler wind light detection and ranging (LIDAR) instrument (A. Dörnbrack, personal communication, 2007).

A significant feature of the composite shown in Figure 11 is the spatial coherence between the lower-level tip jet and the upper-level jet stream. This coherence might be indicative of either (a) a direct dynamical connection in which the tip jet is merely the low-level component of the incident ambient upper-level jet stream supplemented by a contribution due to the flow diversion around the topography, or (b) an indirect relationship whereby the overall synoptic evolution results in both the development and propagation of the low-level cyclone to the lee of Greenland and the alignment of the jet stream overhead of the tip jet. The evolution of the synoptic-scale flow is illustrated by composite vertical

DOI: 10.1002/qj

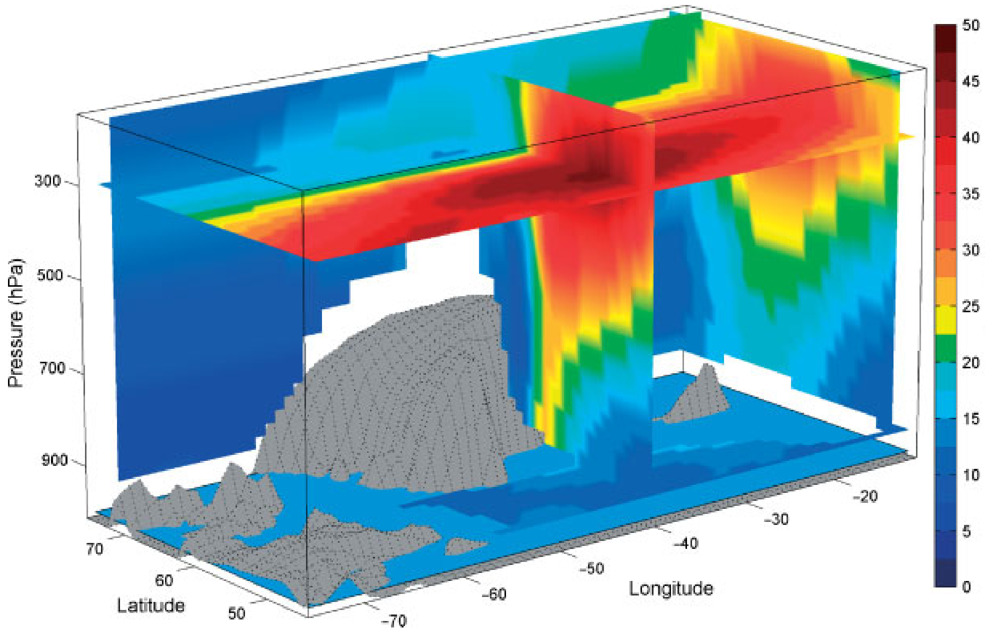

Figure 11. The frame contains a three-dimensional image of the composite ERA-40 wind speed (m s^{-1}) during the most recent (1994–2002) tip jet events. The dominant land mass in the north is Greenland, flanked by Iceland in the east and Baffin Island and Labrador in the west. The tip jet is the tongue of high velocity winds extending down from the maximum aloft near Cape Farewell at the southern tip of Greenland.

cross-sections during the 24 h period surrounding a tip jet event. Figures 12(a) and (c) show that the jet stream both precedes the tip jet and remains after the peak tip jet winds have waned, indicating that the tip jet is not merely a low-level signature of the jet stream.

To consider this aspect further, an examination was undertaken of the contemporaneous occurrence of jet stream and tip jet events. A climatology of jet stream events in the vicinity of southern Greenland was compiled using the approach of Koch *et al.* (2006). This entails identifying when and where the mean wind speed in the range between 100 and 400 hPa exceeds 30 m s^{-1} using the global ERA-40 wind field for the period after the advent of satellite instruments in 1979 (H.Wernli, personal communication, 2007). The associated jet stream frequency field signifies how often a jet stream is present at a grid point. Consideration of this jet stream climatology during tip jet conditions (Figure 13(a)) indicates that tip jet events are almost invariably accompanied by the presence of a jet stream directly south of Greenland. Indeed only two tip jet events (out of 341) were not accompanied by a jet stream being resident within the domain enclosed by the 75% frequency field contour in Figure 13(a). Thus virtually all tip jet events are associated both with a low pressure system generally located east of southern Greenland and a jet stream located directly south of Greenland.

Further insight on this can be gleaned from examining the difference between average winter conditions and those that prevail during tip jet events. Figure 13(b) shows that in general, during winter, the jet stream is present most frequently far to the southwest of Greenland and south of 50°N. However, the anomaly field (Figure 13(c)) clearly shows that during tip jet events the jet stream is present more frequently farther northeastward in the immediate vicinity of southern Greenland. In effect the upper-level jet stream and the lower-level tip jet exist in concert during tip jet events. (Note that the jet stream frequency field anomaly was computed by subtracting the mean winter conditions from the tip jet conditions and then dividing by the standard deviation at each grid point.)

Likewise examination of the difference in the cyclone frequency field between normal winter conditions and those that prevail during tip jet events (Figure 13(d)–(f)) confirm that cyclones are far more often located in the lee of southern Greenland during tip jet events. While all tip jets were associated with a low pressure system in the general vicinity, the significant scatter in positions of the parent lows (Figures 6(b) and 9) reduces the frequency field to below 100%. Also discernible in Figure 13(e) is the signature of the North Atlantic storm track (Hoskins and Hodges, 2002). Moreover, during the winter season, low pressure systems often reside in the neighbourhood of the Irminger Sea (Figure 13(e)) and this reflects in part the climatological signal of the Icelandic Low. Despite the presence of the Icelandic Low, cyclones are so much more prevalent east of southern Greenland during tip jet events that a strong positive frequency field anomaly is evident (Figure 13(f)). Note also the strong negative anomaly south of Greenland that intersects the storm track, also evident in Figure 13(d) as a band of near-zero frequency field south of Greenland. As noted by Våge *et al.* (2008), cyclones in this region do not support the sea level pressure gradient field characteristic of tip jets (note the close spacing of the isobars near Cape Farewell in Figures 1 and 6(b)), and correspondingly this region was devoid of cyclones during those events. The presence of a cyclone south of Greenland is typically associated with easterly tip jet events (Moore, 2003).

DOI: 10.1002/qj

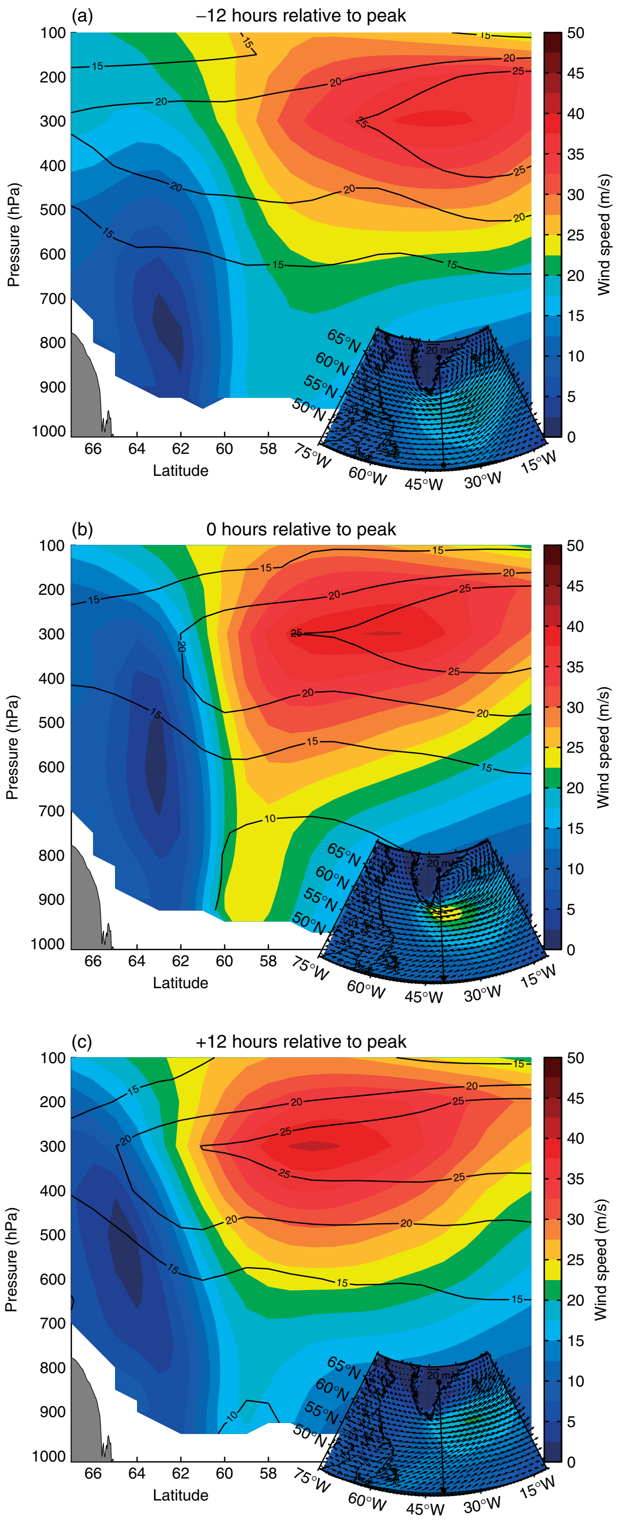

Figure 12. Vertical slices through the composite ERA-40 wind speed during the most recent (1994 to 2002) tip jet events at 40° longitude. The title of each figure refers to the time lag relative to the peak of the composite tip jet. Colours represent the mean wind speed and contours the standard deviation (both m s^{-1}). Greenland is visible in the northern end of the section, and the insets show the mean wind speed and vectors at 800 hPa and the line along which the slice was taken.

In the light of the above results, we can now elaborate on the link between the jet stream and the tip jet. Our results indicate that: (i) the air parcel trajectories entering the tip jet undergo a low-level deflection of flow around Cape Farewell, (ii) the tip jet evolves subsequent to the passage of a low-level synoptic cyclonic system toward Greenland and its arrival over the Irminger Sea, and (iii) the position and evolution of the cyclone is closely related to and influenced by the tropopause-level jet stream. This triple relationship is consistent with the tip jet's occurrence being determined by the combination of the ambient synoptic-scale flow spawning the parent cyclone and steering it to the lee of Greenland, and the subsequent evolution of the low-level jet via orographic effects.

8. Summary and discussion

Westerly tip jets are intense, small-scale wind events that occur frequently east of Cape Farewell, Greenland, during the winter season. A multi-event climatology of tip jets based upon the ERA-40 reanalysis dataset was compiled using an objective and sensitive detection method. For the winters investigated, 1957 to 2002, a total of 586 tip jets were identified, yielding an average of 13 per winter. The diagnostic analysis indicates that (i) the frequency of tip jet occurrence is sensitive both to the NAO index and to the latitude of the Icelandic Low, (ii) the events are short-lived phenomena with mean winds up to 30 m s^{-1} in the core typically lasting about a day, and (iii) during the event cold and dry continental air is advected from the North American continent to the Irminger Sea so that, despite their episodic nature, both the high wind speeds and the strong heat fluxes significantly impact the ocean below (e.g. Pickart *et al.*, 2008).

The present study sheds light on the relative role of two previously described, non-mutually exclusive, mechanisms for the generation of tip jets: (I) blocking of the low-level air upstream of Greenland along with the presence of a low pressure system east of southern Greenland resulting in deflection and acceleration of that blocked air around and downstream of the southern tip of Greenland (Moore and Renfrew, 2005); and (II) orographic descent down the lee slope of Greenland under conservation of the Bernoulli function resulting in an acceleration of the flow (Doyle and Shapiro, 1999). Our diagnostic analysis indicates in line with mechanism (I) that the tip jet air approaches Greenland from the west, is deflected and accelerates around Cape Farewell, and results in a downstream tip jet. Likewise, in line with mechanism (II), there is some indication of descending air over southern Greenland, but this pertains only to a small number of the calculated trajectories.

Our analysis has also revealed an apparently ubiquitous sequence of events that prevails in the run-up to and during a tip jet event. This involves the far-upstream genesis of a synoptic-scale cyclonic system that subsequently tracks to the lee of Greenland, coupled to the contemporaneous arrival of a tropopause-level jet stream immediately to the south of Greenland. The topography of Greenland impacts both the location of the lee-side cyclone and, primarily via mechanism (I), the subsequent evolution of the strong westerly low-level tip jet flow. This sequence of

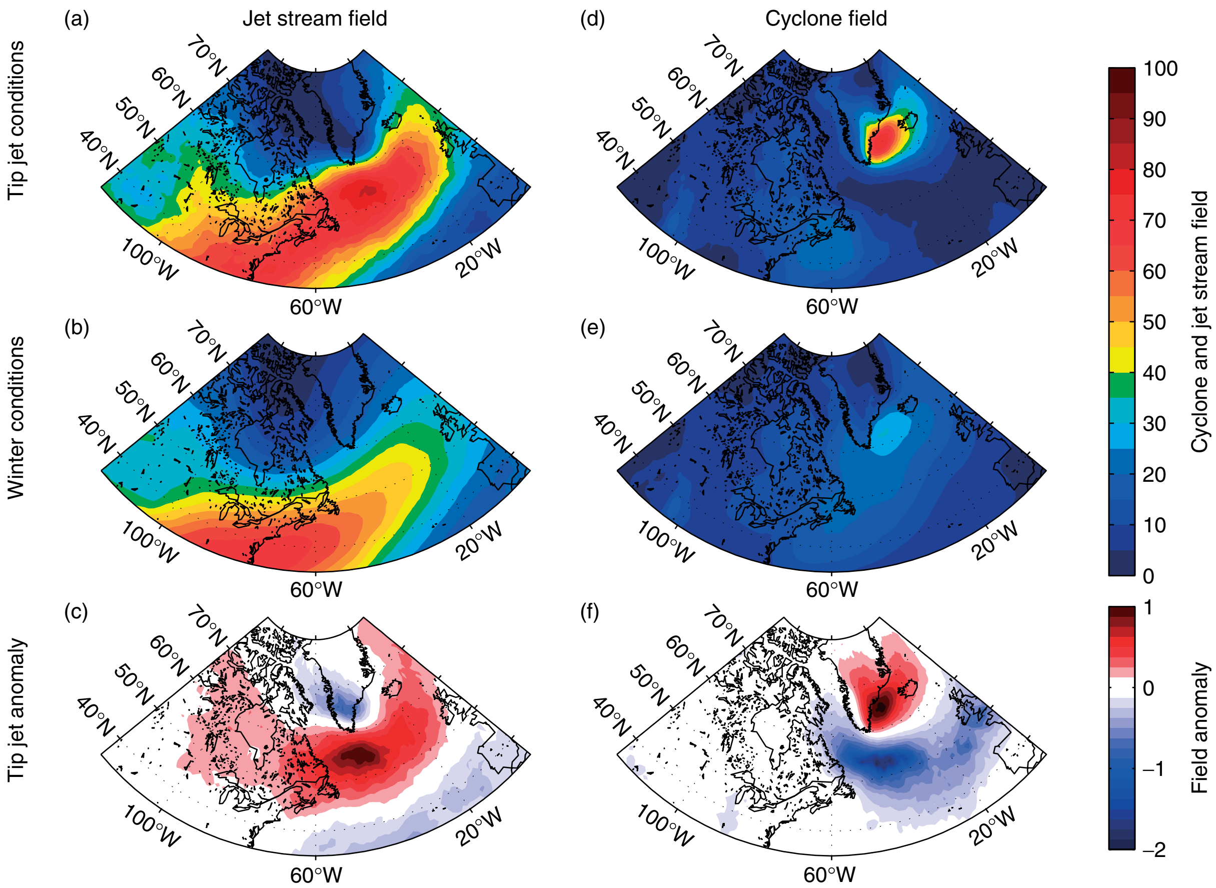

Figure 13. (a, b, c) jet stream and (d, e, f) cyclone frequency fields. (a, d) show tip jet conditions, (b, e) average winter conditions, and (c, f) tip jet anomaly conditions.

events points to the precedence, if not the primacy, of the role and contribution of the lee-side cyclone and the jet stream to the establishment of the tip jet.

A caveat of the ERA-40 reanalysis is its coarse resolution, and it has been shown that an increase in resolution and better representation of the Greenland topography improves the rendition of the tip jet (Jung and Rhines, 2007). Comparison with the QuikSCAT scatterometer winds for the winters of overlap (1999–2002) show that, although their magnitudes were under-represented, most of the tip jets were detected (88%). We also note that the back-trajectories calculated in this study are only as good as the ERA-40 dataset from which they were computed. Present and future reanalyses of higher resolution (such as the North American Regional Reanalysis project; Mesinger *et al.*, 2006) may provide a higher degree of realism. This should improve our understanding of the impact on weather systems by the topography of Greenland, and the myriad of small-scale phenomena that result (e.g. Renfrew *et al.*, 2008).

Finally we note that if a changing climate is accompanied by a poleward shift of the extratropical jet stream, then one might also anticipate an increased frequency in the occurrence of tip jets. This in turn would impact the surface fluxes and air–sea interactions in an already highly sensitive area.

Acknowledgements

The authors wish to thank Harald Sodemann, Heini Wernli, Cornelia Schwierz, Andreas Dörnbrack, Christoph Schär, Jón Egill Kristjánsson, Haraldur Ólafsson and Nicolas Gruber for stimulating discussions. Comments from Ian Renfrew and three anonymous reviewers greatly improved the manuscript. We thank Heini Wernli for assistance with the trajectory model and providing the jet stream database, Cornelia Schwierz for access to the cyclone database, and Sultan Hameed for sharing the COA indices. Access to ECMWF ERA-40 data was provided by MeteoSwiss with help from Dani Lüthi. QuikSCAT data are produced by Remote Sensing Systems and sponsored by the NASA Ocean Vector Winds Science Team. KV was funded in part by the NCCR Climate Programme of the Swiss National Foundation and by grant OCE-0450658 of the National Science Foundation (NSF). RP was supported by NSF grant OCE-0726640.

References

Bakalian F, Hameed S, Pickart RS. 2007. Influence of the Icelandic Low latitude on the frequency of Greenland tip jet events: Implications for Irminger Sea convection. *J. Geophys. Res.* **112**: C04 020, DOI:10.1029/2006JC003 807

Bengtsson L, Hodges KI, Hagemann S. 2004. Sensitivity of the ERA-40 reanalysis to the observing system: Determination of the global

atmospheric circulation from reduced observations. *Tellus* **56A**: 456–471.
Dickson RR, Lazier JRN, Meincke J, Rhines PB, Swift J. 1996. Long-term coordinated changes in the convective activity of the North Atlantic. *Prog. Oceanogr.* **38**: 241–295.
Doyle JD, Shapiro MA. 1999. Flow response to large-scale topography: The Greenland tip jet. *Tellus* **51**: 728–748.
Fairall CW, Bradley EF, Hare JE, Grachev AA, Edson JB. 2003. Bulk parameterization of air-sea fluxes: Updates and verification for the COARE algorithm. *J. Climate* **16**: 571–591.
Hameed S, Shi W, Boyle J, Santer B. 1995. 'Investigation of the centers of action in the North Atlantic and North Pacific in the ECHAM AMIP simulation'. In *Proceedings of the First International AMIP Scientific Conference, Monterey, California. WCRP-92, WMP/TD-732. World Meteorol*. Organization: Geneva.
Hoskins BJ, Hodges KI. 2002. New perspectives on the Northern Hemisphere winter storm tracks. *J. Atmos. Sci.* **59**: 1041–1061.
Hurrell JW. 1995. Decadal trends in the North Atlantic Oscillation: Regional temperatures and precipitation. *Science* **269**: 676–679.
Jung T, Rhines PB. 2007. Greenland's pressure drag and the Atlantic storm track. *J. Atmos. Sci.* **64**: 4004–4030, DOI: 10.1175/2007JAS2216.1
Kalnay E, Kanamitsu M, Kirtler R, Collins W, Deaven D, Gandin L, Iredell M, Saha S, White G, Woollen J, Zhu Y, Chelliah M, Ebisuzaki W, Higgins W, Janowiak J, Mo KC, Ropelewski C, Wang J, Leetma A, Reynolds R, Jenne R, Joseph D. 1996. The NCEP/NCAR 40-year reanalysis project. *Bull. Am. Meteorol. Soc.* **77**: 437–471.
Koch P, Wernli H, Davies HC. 2006. An event-based jet-stream climatology and typology. *Int. J. Climatol.* **26**: 283–301.
Kristjánsson JE, McInnes H. 1999. The impact of Greenland on cyclone evolution in the North Atlantic. *Q. J. R. Meteorol. Soc.* **125**: 2819–2834.
Kristjánsson JE, Thorsteinsson S. 2009. Phase-locking of a rapidly developing extratropical cyclone by Greenland's orography. *Q. J. R. Meteorol. Soc.* **135**: 1986–1998.
Lavender KL, Davis RE, Owens WB. 2000. Mid-depth recirculation observed in the interior Labrador and Irminger Seas by direct velocity measurements. *Nature* **407**: 66–69.
McCauley MP, Sturman AP. 1999. A study of orographic blocking and barrier wind development upstream of the Southern Alps, New Zealand. *Meteorol. Atmos. Phys.* **70**: 121–131.
McInnes H, Kristjánsson JE, Schyberg H, Røsting B. 2009. An assessment of a Greenland lee cyclone during the Greenland Flow Distortion experiment – An observational approach. *Q. J. R. Meteorol. Soc.* **135**: 1968–1985.
Mesinger F, DiMego G, Kalnay E, Mitchell K, Shafran PC, Ebisuzaki W, Jović D, Woollen J, Rogers E, Berbery EH, Ek MB, Fan Y, Grumbine R, Higgins W, Li H, Lin Y, Manikin G, Parrish D, Shi W. 2006. North American regional reanalysis. *Bull. Am. Meteorol. Soc.* **87**: 343–360.
Moore GWK. 2003. Gale force winds over the Irminger Sea to the east of Cape Farewell, Greenland. *Geophys. Res. Lett.* **30**: 1894, DOI: 10.1029/2003GLO18 012
Moore GWK, Renfrew IA. 2005. Tip jets and barrier winds: A QuikSCAT climatology of high wind speed events around Greenland. *J. Climate* **18**: 3713–3725.
Moore GWK, Pickart RS, Renfrew IA. 2008. Buoy observations from the windiest location in the world ocean, Cape Farewell, Greenland. *Geophys. Res. Lett.* **35**: L18 802, DOI: 10.1029/2008GL034 845
Ólafsson H, Bougeault P. 1996. Nonlinear flow past an elliptic mountain ridge. *J. Atmos. Sci.* **53**: 2465–2489.
Parish TR. 1982. Barrier winds along the Sierra Nevada mountains. *J. Appl. Meteorol.* **21**: 925–930.
Petersen GN, Ólafsson H, Kristjánsson JE. 2003. Flow in the lee of idealized mountains and Greenland. *J. Atmos. Sci.* **60**: 2183–2195.
Petersen GN, Kristjánsson JE, Ólafsson H. 2004. Numerical simulations of Greenland's impact on the Northern Hemisphere winter circulation. *Tellus* **56A**: 102–111.
Petersen GN, Renfrew IA, Moore GWK. 2009. An overview of barrier winds off southeastern Greenland during GFDex. *Q. J. R. Meteorol. Soc.* **135**: 1950–1967.
Pickart RS, Spall MA, Ribergaard MH, Moore GWK, Milliff RF. 2003a.. Deep convection in the Irminger Sea forced by the Greenland tip jet. *Nature* **424**: 152–156.
Pickart RS, Straneo F, Moore GWK. 2003b.. Is Labrador Sea Water formed in the Irminger Basin? *Deep-Sea Res. Part I* **50**: 23–52.
Pickart RS, Våge K, Moore GWK, Renfrew IA, Ribergaard MH, Davies HC. 2008. Convection in the western North Atlantic sub-polar gyre: Do small-scale wind events matter? In *Arctic-Subarctic Ocean Fluxes: Defining the role of the northern seas in climate*. Dickson RR, Meincke J, Rhines P (eds). Springer: Dordrecht, The Netherlands; pp 629–652.
Pierrehumbert RT, Wyman B. 1985. Upstream effects of mesoscale mountains. *J. Atmos. Sci.* **42**: 977–1003.
Renfrew IA, Moore GWK, Guest PS, Bumke K. 2002. A comparison of surface layer and surface turbulent flux observations over the Labrador Sea with ECMWF analyses and NCEP reanalyses. *J. Phys. Oceanogr.* **32**: 383–400.
Renfrew IA, Moore GWK, Kristjánsson JE, Ólafsson H, Gray SL, Petersen GN, Coauthors. 2008. The Greenland flow distortion experiment. *Bull. Am. Meteorol. Soc.* **89**: 1307–1324.
Renfrew IA, Petersen GN, Sproson DAJ, Moore GWK, Adiwidjaja H, Zhang S, North R. 2009. A comparison of aircraft-based surface-layer observations over Denmark Strait and the Irminger Sea with meteorological analyses and QuikSCAT winds. *Q. J. R. Meteorol. Soc.* **135**: 2046–2066.
Sampe T, Xie SP. 2007. Mapping high sea winds from space. *Bull. Am. Meteorol. Soc.* **88**: 1965–1978.
Schär C. 1993. A generalization of Bernoulli's theorem. *J. Atmos. Sci.* **50**: 1437–1443.
Schwerdtfeger W. 1975. The effect of the Antarctic Peninsula on the temperature regime of the Weddell Sea. *Mon. Weather Rev.* **103**: 45–51.
Seefeldt MW, Cassano JJ. 2008. An analysis of low-level jets in the greater Ross Ice Shelf region based on numerical simulations. *Mon. Weather Rev.* **136**: 4188–4205.
Skeie RB, Kristjánsson JE, Ólafsson H, Røsting B. 2006. Dynamical processes related to cyclone development near Greenland. *Meteorol. Zeitschrift* **15**: 147–156, DOI: 10.1127/0941–2948/2006/0114
Smith RB. 1989. Hydrostatic flow over mountains. In *Advances in Geophysics*, **31**: Academic Press: pp 1–41.
Spall MA, Pickart RS. 2003. Wind-driven recirculations and exchange in the Labrador and Irminger Seas. *J. Phys. Oceanogr.* **33**: 1829–1845.
Sproson DAJ, Renfrew IA, Heywood KJ. 2008. Atmospheric conditions associated with oceanic convection in the south-east Labrador Sea. *Geophys. Res. Lett.* **35**: L06 601, DOI: 10.1029/2007GL032 971
Tsukernik M, Kindig D, Serreze MC. 2007. Characteristics of winter cyclone activity in the northern North Atlantic: Insights from observations and regional modeling. *J. Geophys. Res.* **112**: D03 101, DOI: 10.1029/2006JD007 184
Uppala SM, Kållberg PW, Simmons AJ, Andrae U, Da Costa Bechtold V, Fiorino M. Gibson JK, Haseler J, Hernandez A, Kelly GA, Li X, Onogi K, Saarinen S, Sokka N, Allan RP, Andersson E, Arpe K, Balmaseda MA, Beljaars ACM, Van de Berg L, Bidlot J, Bormann N, Caires S, Chevallier F, Dethof A, Dragosazac M, Fisher M, Fuentes M, Hagemann S, Hólm E, Hoskins BJ, Isaksen L, Janssen PAEM, Jenne R, McNally AP, Mahfouf J-E, Morcrette J-J, Rayner NA, Saunders RW, Simon P, Sterl A, Trenberth KA, Untch A, Vasiljevic D, Viterbo P, Woollen J. 2005. The ERA40 re-analysis. *Q. J. R. Meteorol. Soc.* **131**: 2961–3012.
Våge K, Pickart RS, Moore GWK, Ribergaard MH. 2008. Winter mixed-layer development in the central Irminger Sea: The effect of strong, intermittent wind events. *J. Phys. Oceanogr.* **38**: 541–565.
Våge K, Pickart RS, Thierry V, Reverdin G, Lee CM, Petrie B, Agnew TA, Wong A, Ribergaard MH. 2009. Surprising return of deep convection to the subpolar North Atlantic Ocean in winter 2007–2008. *Nature Geoscience* **2**: 67–72, DOI: 10.1038/NGEO382.
Wentz FJ, Smith DK, Mears CA, Gentemann CL. 2001. 'Advanced algorithms for QuikScat and SeaWinds/AMSR'. In *Proceedings of IGARSS'01, Sydney, Australia, 9–13 July 2001.* **3**: 1079–1081.
Wernli H, Davies HC. 1997. A Lagrangian-based analysis of extratropical cyclones. I: The method and some applications. *Q. J. R. Meteorol. Soc.* **123**: 467–489.
Wernli H, Schwierz C. 2006. Surface cyclones in the ERA-40 dataset (1958–2001), Part I: Novel identification method and global climatology. *J. Atmos. Sci.* **63**: 2486–2507.